Compact Modeling of the Threshold Voltage in Silicon Nanowire MOSFET including 2D-Quantum Confinement Effects

Jean-Luc Autran, Karim Nehari, Daniela Munteanu

Molecular Simulation
Journal of
Experimental Nanoscience

Taylor & Francis
Taylor & Francis Group

Compact Modeling of the Threshold Voltage in Silicon Nanowire MOSFET including 2D-Quantum Confinement Effects

Journal:	*Molecular Simulation/Journal of Experimental Nanoscience*
Manuscript ID:	GMOS-2005-0021.R1
Journal:	Molecular Simulation
Date Submitted by the Author:	11-Aug-2005
Complete List of Authors:	AUTRAN, Jean-Luc; L2MP-CNRS, Bat. IRPHE Nehari, Karim; L2MP-CNRS, Bat. IRPHE Munteanu, Daniela; L2MP-CNRS, Bat. IRPHE
Keywords:	2D-quantum confinement effects, threshold voltage, quantum nanowire MOSFET, compact modeling, 3D numerical simulation

Compact Modeling of the Threshold Voltage in Silicon Nanowire MOSFET including 2D-Quantum Confinement Effects

J.L. Autran[*,+], K. Nehari, D. Munteanu

L2MP, UMR CNRS 6137

Bâtiment IRPHE, 49 rue Joliot-Curie, BP 146, F-13384 Marseille Cedex 13, France

([+]also with Institut Universitaire de France – IUF)

[*]Corresponding author :

Prof. Jean-Luc AUTRAN

L2MP, UMR CNRS 6137
Bâtiment IRPHE – BP 146
49, rue Joliot Curie
F-13384 MARSEILLE Cedex 13, France

Phone :+33 4 96 13 97 17
Fax : +33 4 96 13 97 09
E-mail : autran@newsup.univ-mrs.fr

ABSTRACT

A quantum-mechanical compact model of the threshold voltage (V_T) for quantum nanowire MOSFETs has been developed. This approach is based on analytical solutions for the decoupled 2D Schrödinger and 1D Poisson equations solved in the silicon channel. A quantum correction based on the perturbation theory has been also introduced to improve the model accuracy. Finally, the validity of the model has been verified by comparison with data obtained with a 2D/3D Poisson-Schrödinger drift-diffusion simulation code.

Keywords: compact modeling, threshold voltage, quantum nanowire MOSFET, 2D-quantum confinement effects, 3D numerical simulation

1. Introduction

Multi-gate MOS transistors are widely recognized as one of the most promising solutions for meeting the roadmap requirements in the deca-nanometer scale of device integration [1]. **Recently, these architectures are also presenting a growing interest for the integration of post-conventional Silicon devices and molecular-based devices, since the active region of the transistor, i.e. the conduction channel, can be alternatively played by a semiconductor nanowire, a Carbon nanotube, a molecule or an atomic linear chain [2-3]. In all cases, these structures exhibit a superior control of short channel effects resulting from an exceptional electrostatic coupling between the conduction channel and the surrounding gate electrode.**

In the case of Silicon-based CMOS technologies, a wide variety of multi-gate architectures, including Double-Gate (DG), Gate-All-Around (GAA), PiFET, FinFET, Rectangular or Cylindrical nanowire MOSFETs, linear atomic-chain transistors has been proposed in the recent literature [1-2]. For all these structures, one of the identified challenges remains the development of compact models taking into account the main physical phenomena governing the devices at this scale of integration.

In this work, a compact model for the threshold voltage (V_T) of long-channel quantum Si nanowire (QW) MOSFETs is developed. Schematic representations of different QW architectures are shown in Fig. 1. In such devices for which the lateral dimensions, i.e. the Si film thickness and its width, are ultimately downscaled to a few nanometers, quantum-mechanical carrier confinement effects are exacerbated in the two (y- and z-) directions perpendicular to the transport one (x-). As we will detail in the following, our present approach is thus based on the decoupled solution of the Poisson and Schrödinger equations in the (y,z) plane of the structure. Threshold voltage obtained from this new model will be

confronted with data directly calculated using a 2D/3D quantum-mechanical simulation code coupling the Poisson-Schrödinger system with the Drift-Diffusion transport equation (Balmos3D).

2. Threshold voltage modeling

2.1. V_T definition and criterion

The band diagram in the vertical (y-) direction (middle of the structure) for a n-channel QW transistor is schematically represented in Fig. 2. The potential reference is assumed to be the electron Fermi level of the n+ source region. The potential, Ψ, is defined as the band bending with respect to the intrinsic Fermi level in the silicon film. It is important to note that the surface potential, Ψ_s, as defined here, is different from the surface potential in conventional bulk MOSFET, Ψ_{sc}, which is given by the band bending between the silicon surface and the substrate volume. The relation between the two potentials is $\Psi_{sc}=\Psi_s+\phi_F$ where $\phi_F=(kT/q)\ln(N_A/n_i)$ is the Fermi potential, N_A is the film doping and n_i is the intrinsic carrier concentration. In conventional MOSFET, the threshold voltage is usually defined as the gate voltage necessary for obtaining a band bending of $\Psi_{sc}=2\phi_F$, which means $\Psi_s=\phi_F$. This definition does no more apply to QW MOSFET: our extensive numerical simulation fully confirms this remark and shows that surface potential at threshold, Ψ_s^T, is different from ϕ_F. Other definitions for V_T exist, as derived from the constant-current method or the maximum of $\partial^2 I_D/\partial V_G^2$. In a recent work [4], we used this latter criterion, but the resulting analytical expression of the threshold voltage is quite complicated and its demonstration demands heavy mathematical manipulations. For obtaining a more simple expression of V_T, we consider here the well-known definition where V_T is the gate voltage for which the

inversion charge Q_{iT} in the transistor channel (inversion charge at threshold) is given by [4,5]:

$$Q_{iT} \cong (V_G - V_T)C_{ox} = \frac{kT}{q}C_{ox} \quad (1)$$

where V_G-V_T is assumed to be ~kT/q around threshold. We verified that this value of Q_{iT} is very close to the inversion charge obtained by the numerical simulation of multi-gate structures with different channel doping levels, channel thicknesses and gate oxide thicknesses.

Once the inversion charge at threshold has been defined, the determination of V_T can be easily conducted in two steps: i) express this inversion charge (Q_i) in the QW channel as a function of V_G and ii) numerically solve the equation $Q_i(V_G)=Q_{iT}$. In the following, the calculation of Q_i is obtained from the decoupled solution of the Poisson equation and Schrödinger equations. The first equation leads to the band bending profile in the Si film; the second one gives energy levels in the QW (considered as a 2D quantum-well) used to evaluate the inversion charge.

2.2. Device electrostatics

Considering a multi-gate QW structure represented in Fig. 1, our approach is based on a parabolic approximation of the vertical (y-) potential distribution in the film at threshold, which has been fully confirmed by numerical simulation in previous studies [4,6]. This result can be, of course, generalized for the other direction (z-axis) perpendicular to the channel axis. We can write:

$$\Psi = \Psi_s - \beta\, t_{Si}\, y + \beta\, y^2 \quad (2)$$

With definitions in Fig. 1 and applying the Gauss law, the boundary conditions at the two oxide/silicon interfaces are identical and give:

$$V_G - V_{FB} = \frac{\varepsilon_{Si}}{\varepsilon_{ox}} t_{ox} E + \Psi_s + \phi_F \quad (4)$$

where V_{FB} is the flat band voltage, ε_{Si} and ε_{ox} are the silicon and oxide permitivities, respectively, t_{ox} is the oxide thickness and E is the electric field at the interface:

$$E = -\frac{d\Psi}{dy}\Big|_{y=0} = \beta t_{Si} \quad (5)$$

Expressions (2) to (5) form a complete set of equations to analytically evaluate the band bending profile in the silicon film under threshold condition. As shown in Fig. 3 in comparison with numerical simulation, relation (2) is a very good approximation for the potential distribution in the film at threshold for various doping levels. The potential is symmetric with respect to the middle of the silicon film and has a quasi-parabolic dependence.

2.3. Quantum-mechanical evaluation of the inversion charge

The second step of our model consists in calculating the inversion charge in the silicon quantum-wire. In a first approach, this QW can be simply depicted as a 2D quantum-well with infinite walls, for example a rectangular well for DG or GAA structures, a cylindrical well for the cylindrical QW transistor (Fig. 1), etc. The calculations are developed here for the rectangular infinite well (i.e. the GAA structure) with carriers confined in the (y,z) plane. Assuming, in a first approximation, that the conduction band profile is flat inside the well, simple analytical expression for the quantum energy levels can be used. In the particular case of <100>-oriented Silicon, three different series of quantum energy levels

must be considered in the evaluation of the inversion charge, to properly take into account the effective mass ellipsoid characteristics (see Fig. 4):

$$\begin{cases} E_1(i,j) = \dfrac{\pi^2\hbar^2 i^2}{m_l t_{Si}^2} + \dfrac{\pi^2\hbar^2 j^2}{m_t W^2} \\ E_2(i,j) = \dfrac{\pi^2\hbar^2 i^2}{m_t t_{Si}^2} + \dfrac{\pi^2\hbar^2 j^2}{m_l W^2} \\ E_3(i,j) = \dfrac{\pi^2\hbar^2 i^2}{m_t t_{Si}^2} + \dfrac{\pi^2\hbar^2 j^2}{m_t W^2} \end{cases} \quad (6)$$

where $m_l \approx 0.916 \times m_0$ and $m_t \approx 0.19 \times m_0$ are the longitudinal and transversal effective mass of electrons, respectively.

For each energy level $E_k(i,j)$, referenced with respect to the bottom of the quantum-well, the contribution to the total charge integrated over the Si film cross-section ($W \times t_{Si}$) is:

$$n(E_k, i, j) = 2 \times \int_{E_k}^{+\infty} \rho_{1D}(E, E_k) f(E) dE \quad (7)$$

where the factor 2 accounts for the number of equivalent valleys, $\rho_{1D}(E,E_k)$ is the 1D density-of-states and f(E) is the Fermi-Dirac distribution function:

$$\rho(E, E_k) = \frac{1}{\pi}\left(\frac{2m_D}{\hbar^2}\right)^{1/2} \frac{1}{\sqrt{E - E_k}} \quad (8)$$

$$f(E) = \frac{1}{1 + \exp\left(\dfrac{E - E_F}{kT}\right)} \quad (9)$$

where m_D is the 1D density-of-states effective mass ($m_D=m_t$ for k=1,2 and $m_D=m_l$ for k=3). In Eq. (7), the calculated charge depends on V_G via the position of the Fermi level with respect to the bottom of the conduction band (assimilated to the bottom of the quantum well) and thus with respect to the different energy levels. The inversion charge to be considered for V_T determination using $Q_i(V_G)=Q_i^T$ is finally:

$$Q_i(V_G) = q\sum_k \sum_i \sum_j n(E_k, i, j) \quad (10)$$

In order to enhance the accuracy of the model, a first-order perturbation correction of the energy levels given by Eq. (6) has been conducted [6,7]. The Hamiltonian V of the perturbation is simply evaluated from the electrostatic potential profile (Eq. (2)), assuming that a similar profile is obtained in the second perpendicular direction:

$$V(y,z) = \beta_y y(t_{Si} - y) + \beta_z z(W - z) \quad (11)$$

where β_y and β_z are two constants depending on β.

The first-order correction to apply to the energy levels in the well is given by:

$$\Delta E^{i,j} = \left\langle \varphi^{i,j} \middle| V \middle| \varphi^{i,j} \right\rangle \quad (12)$$

with $\varphi^{i,j}$ is the wave function related to levels defined with quantum numbers i and j:

$$\varphi^{i,j}(y,z) = \sqrt{\frac{2}{tSi}} \sin\left(\frac{i\pi y}{t_{Si}}\right) \cdot \sqrt{\frac{2}{W}} \sin\left(\frac{j\pi z}{W}\right) \quad (13)$$

An analytical evaluation of $\Delta E^{i,j}$ immediately gives:

$$\Delta E^{i,j} = \iint_{W \times tSi} \left[\varphi^{i,j}(y,z)\right]^2 V(y,z)dydz = \frac{\beta_y t_{Si}^2}{6}\left(1 + \frac{3}{i^2\pi^2}\right) + \frac{\beta_z W^2}{6}\left(1 + \frac{3}{j^2\pi^2}\right) \quad (14)$$

The corrected energy levels to be considered in Eq. (10) for the evaluation of Q_i are finally:

$$\tilde{E}_k(i,j) = E_k(i,j) + \Delta E^{i,j} \quad (15)$$

3. Model validation and discussion

The present model has been validated by comparison with numerical simulation using a 2D/3D quantum-mechanical simulation code coupling the Poisson-Schrödinger system with the Drift-Diffusion transport equation (Balmos3D, [8]). First, considering a single

direction for carrier confinement (t_{Si} downscaling at fixed infinitely large W). Fig. 6 shows that a very good match is obtained between analytical and 2D numerical results in a rectangular QW structure. In particular, it is shown that the model is able to very well predict the dependence of V_T with t_{Si} and also with N_A. In a second step, both y- and z-directions for carrier confinement have been considered and the compact model has been validated using 3D numerical simulation, as shown in Fig. 7. One again the fit between compact model and numerical data is very satisfactory. Fig. 7 and Fig. 8 show that the threshold voltage increase, due to carrier confinement in the z-direction, becomes significant for W lower than ~20nm. It is also interesting to remark that, when W is scaled down, the threshold voltage increase becomes more important as long as the film thickness decreases. Indeed, when switching from 1D to 2D confinement, the threshold voltage increase is more pronounced due not only to the increase of the distance between the energy levels and the Fermi level, but in the same time, to the change of the density-of-states. In other words, the band bending must be accentuated to obtain the same inversion charge with higher energy levels and lower number of quantum states per level. Finally, Fig. 9 shows the variations of V_T predicted by the compact model as a function of both W and t_{Si} for a rectangular GAA QW.

4. Conclusion

In conclusion, a compact modeling of the threshold voltage for quantum-wire MOSFETs has been developed. The model, based on analytical solutions for the decoupled Schrödinger and Poisson equations, also integrates a quantum correction based on the perturbation theory to improve the evaluation of the inversion charge in the film. The validity of this approach has been demonstrated by comparison with 3D numerical

simulation. Finally this work provides an analytical and useful way for the threshold voltage evaluation in such nanodevices with a unified formalism employed in both classical and quantum-mechanical approaches.

ACKNOWLEDGMENTS

This work is supported by the European Commission in the framework of the Network of Excellence on Silicon-based nanodevices (SINANO, contract IST-506844).

REFERENCES

[1] For a recent review, see D. Hisamoto, Short course IEDM 2003 and references therein.

[2] M. Bescond *et al.*, "3D Quantum Modeling and Simulation of Multiple-Gate Nanowire MOSFETs", IEDM Tech. Dig., 617 (2004).

[3] M. Bescond *et al.*, "Atomic-scale modeling of Double-Gate MOSFETs using a tight-binding Green's function formalism", Solid-State Electron. 48, 567 (2004).

[4] D. Munteanu *et al.*, "Unified Analytical Model of Threshold Voltage in Symmetric and Asymmetric Double-Gate MOSFETs", Proc. ULIS, p. 35-38 (2003).

[5] S. Harrison *et al.*, "Electrical characterization and modelling of high-performance SON DG MOSFETs", Proc. ESSDERC, 373 (2004).

[6] J.L. Autran *et al.*, "Quantum-Mechanical Analytical Modeling of Threshold Voltage in Long-Channel Double-Gate MOSFET with Symmetric and Asymmetric Gates", Nanotech 2004 Proc., Vol. 2, p. 163-166 (2004).

[7] G. Baccarani *et al.*, "A Compact Double-Gate MOSFET Model Comprising Quantum-Mechanical and Nonstatic Effects", IEEE Trans. Electron Dev. **46**, 1656 (1999).

[8] Balmos3D simulation code, L2MP-CNRS (2003).

FIGURE CAPTIONS

Figure 1. Schematic representation of different architectures envisaged for the Si nanowire MOSFET. The main geometrical key-parameters of the devices are defined.

Figure 2: Schematic band diagram for a QW transistor in the y-direction (middle part of the device) and definition of internal potential and energy levels.

Figure 3: Potential distribution in the silicon film at threshold in a symmetric DG-QW structure for different doping levels as calculated by the analytical model and numerically solved from Poisson equation.

Figure 4: Schematic illustration of electron confinement in a Silicon quantum-wire with a rectangular cross-section ($W \times t_{Si}$).

Figure 5: Illustration of the first-order perturbation method used to correct energy level values in the 2D rectangular well of the QW MOSFET.

Figure 6. Quantum V_T predicted by the analytical model in an infinitely large DG-QW structure for two different doping levels. Comparison with 2D quantum-mechanical numerical simulation is also reported.

Figure 7. Quantum V_T predicted by the analytical model as a function of W and t_{Si} for a rectangular GAA QW. Comparison with 3D quantum numerical simulation.

Figure 8. ΔV_T predicted by the analytical model as a function of the channel width in thick and very thin films, illustrating the contributions of 1D and 2D confinements in the threshold voltage shift between quantum (V_{Tq}) and classical (V_{Tcl}) threshold voltage.

Figure 9. $V_T(W,t_{Si})$ surface map for a rectangular GAA QW long-channel transistor (L=100nm, V_{DS}=50mV, $N_A=10^{16}$ cm^{-3}) as calculated by the proposed model.

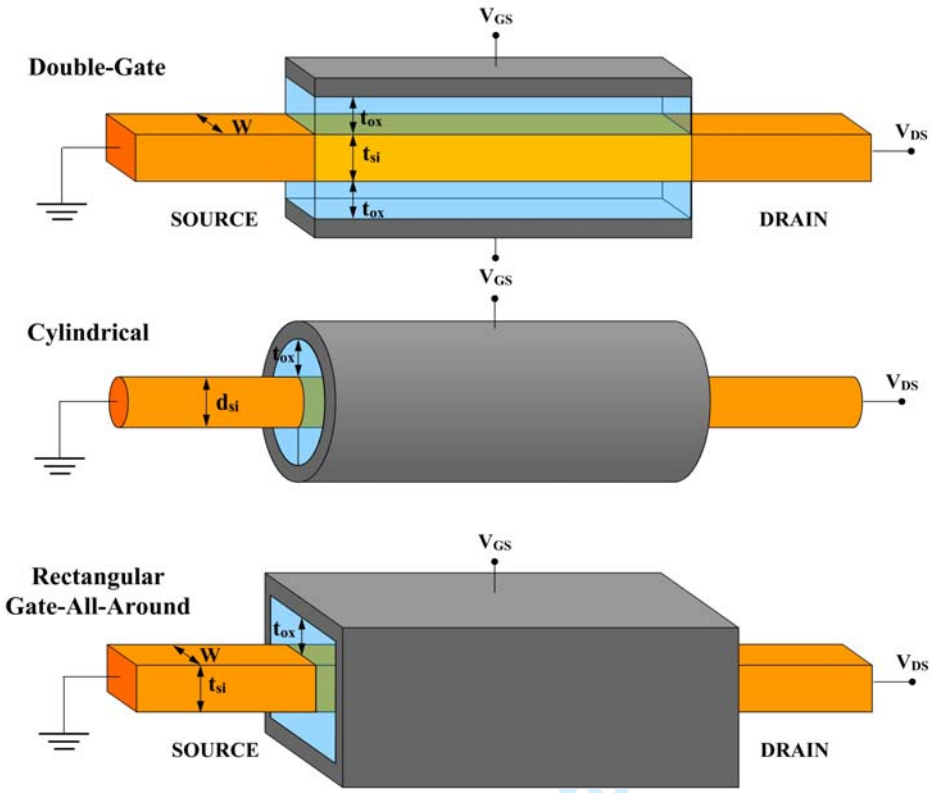

Figure 1.

Autran et al.

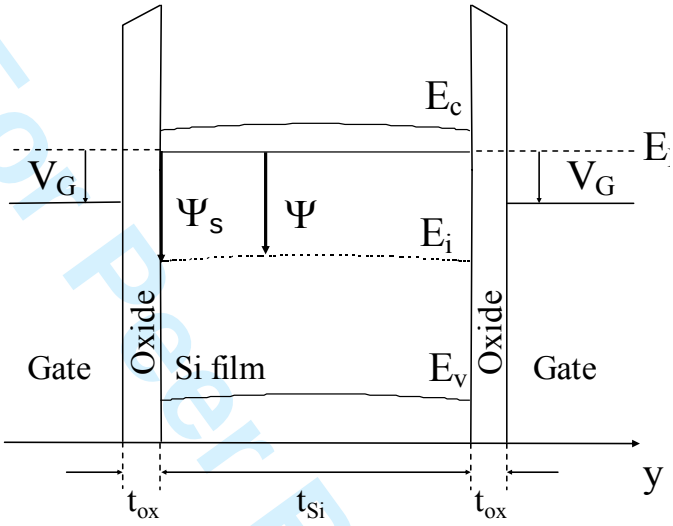

Figure 2.

Autran et al.

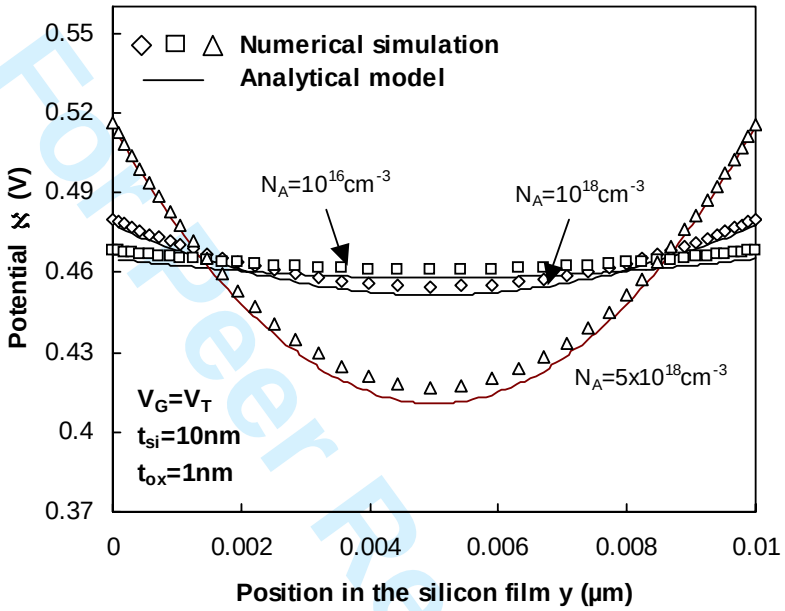

Figure 3.

Autran et al.

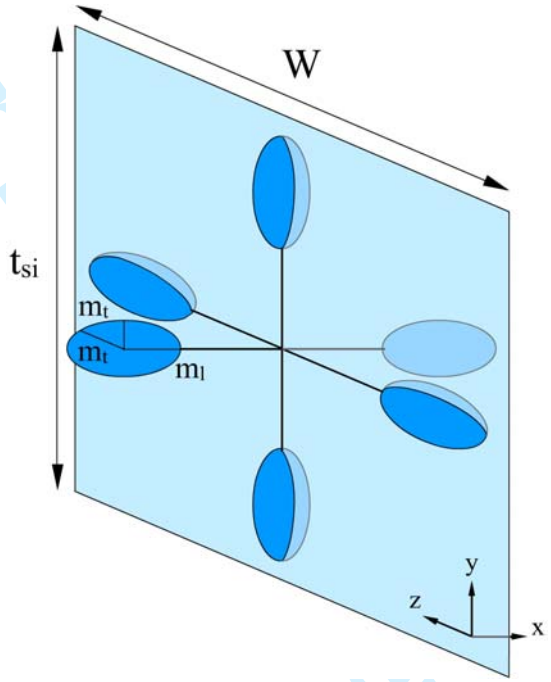

Figure 4.

Autran et al.

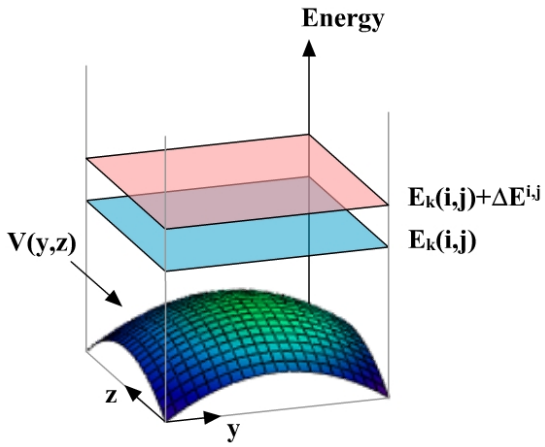

Figure 5.

Autran et al.

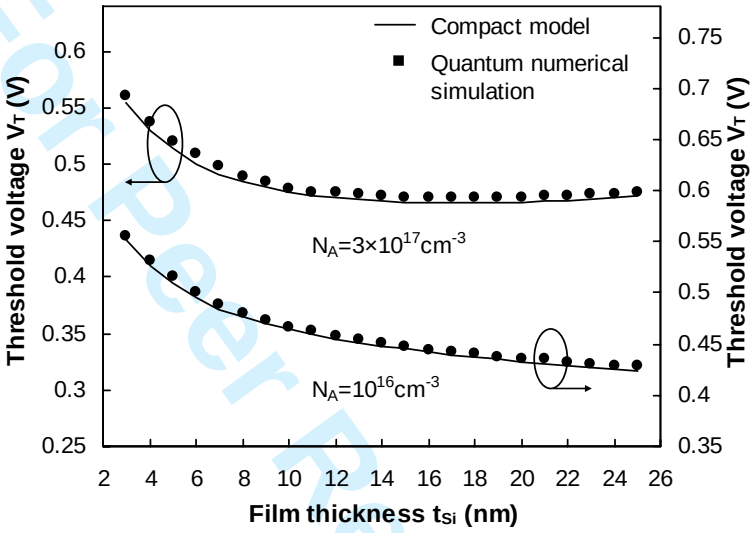

Figure 6.

Autran et al.

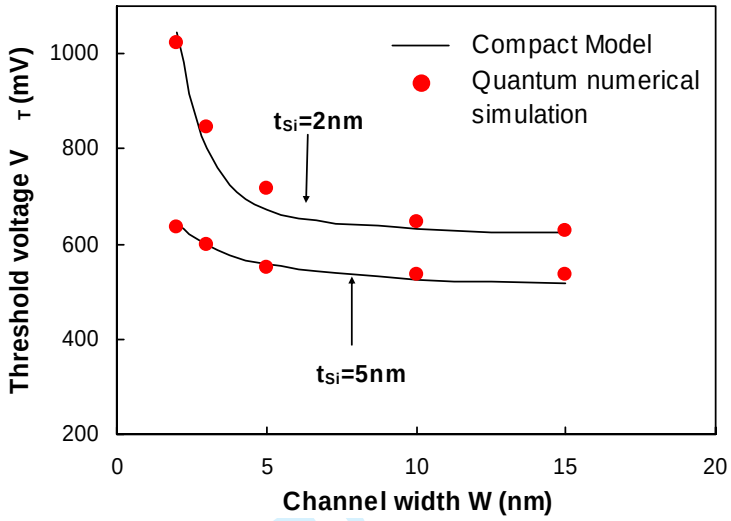

Figure 7.

Autran et al.

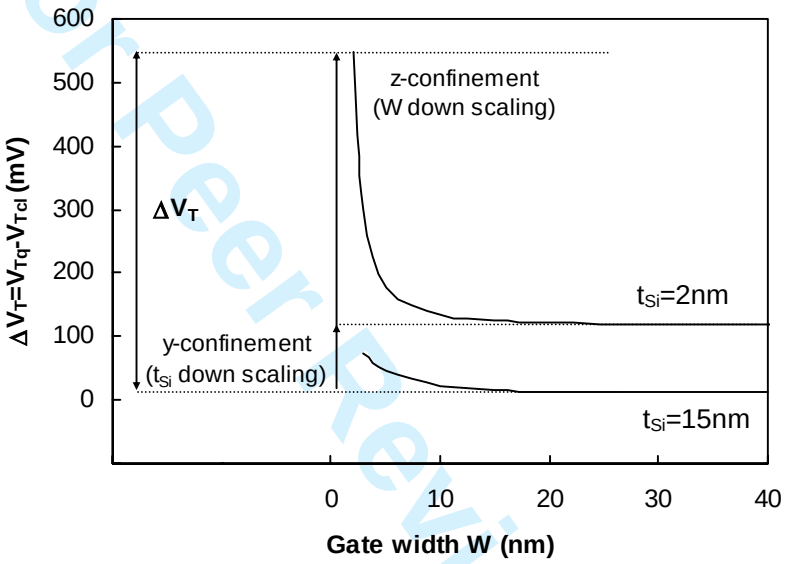

Figure 8.

Autran et al.

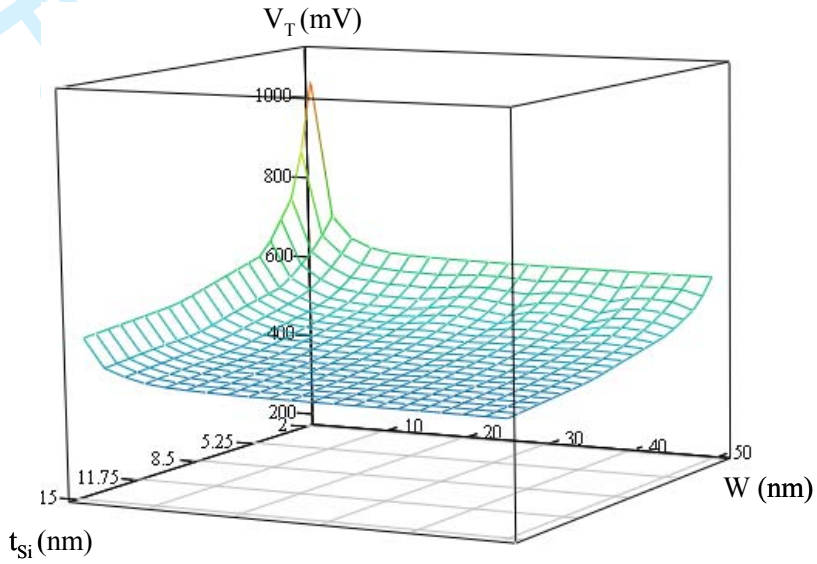

Figure 9.

Autran et al.